Article

Nanopatterned Bulk Metallic Glass Biosensors

Emily R. Kinser, Jagannath Padmanabhan, Roy Yu, Sydney L. Corona, Jinyang Li, Sagar Vaddiraju, Allen Legassey, Ayomiposi Loye, Jenna Balestrini, Dawson A. Solly, Jan Schroers, Andre D. Taylor, Fotios Papadimitrakopoulos, Raimund I Herzog, and Themis R. Kyriakides

ACS Sens., **Just Accepted Manuscript** • DOI: 10.1021/acssensors.7b00455 • Publication Date (Web): 08 Nov 2017

ACS Sensors is published by the American Chemical Society. 1155 Sixteenth Street N.W., Washington, DC 20036

NANOPATTERNED BULK METALLIC GLASS BIOSENSORS

*Emily R. Kinser,†§^ Jagannath Padmanabhan,†‡ Roy Yu,^ Sydney L. Corona,† Jinyang Li,†|| Sagar Vaddiraju,± Allen Legassey,± Ayomiposi Loye, †‡ Jenna Balestrini,† Dawson A. Solly,† Jan Schroers,†§ André D. Taylor,†|| Fotios Papadimitrakopoulos,±# Raimund I. Herzog,º and Themis R. Kyriakides †‡¥**

† Center for Research on Interface Structures and Phenomena, Yale University, New Haven, Connecticut 06520, United States,

§ Department of Mechanical Engineering and Materials Science, Yale University, New Haven, Connecticut 06520, United States,

^ IBM Thomas J. Watson Research Center, Yorktown Heights, New York 10598, United States,

‡ Department of Biomedical Engineering, Yale University, New Haven, Connecticut 06520, United States,

|| Department of Chemical and Environmental Engineering, Yale University, New Haven, Connecticut 06520, United States,

± Biorasis Inc., Storrs, Connecticut 06269, United States,

Department of Chemistry, Institute of Materials Science, University of Connecticut, Connecticut 06269, United States

º Department of Internal Medicine, Yale University, New Haven, Connecticut 06520, United States,

¥ Department of Pathology, Yale University, New Haven, Connecticut 06520, United States,

KEYWORDS: bulk metallic glass, electrochemical biosensor, biomaterials, nanorods, nanotopography.

ABSTRACT: Nanopatterning as a surface area enhancement method has potential to increase signal and sensitivity of biosensors. Platinum-based bulk metallic glass (Pt-BMG) is a biocompatible material with electrical properties conducive for biosensor electrode applications, which can be processed in air at comparably low temperatures to produce non-random topography at the nanoscale. Work presented here employs nanopatterned Pt-BMG electrodes functionalized with glucose oxidase enzyme to explore the impact of non-random and highly reproducible nanoscale surface area enhancement on glucose biosensor performance. Electrochemical measurements including cyclic voltammetry (CV) and amperometric voltammetry (AV) were completed to compare the performance of 200nm Pt-BMG electrodes vs. Flat Pt-BMG control samples. Glucose dosing response was studied in a range of 2mM to 10mM. Effective current density dynamic range for the 200nm Pt-BMG was 10-12X greater than that of the Flat BMG control. Nanopatterned electrode sensitivity was measured to be

3.28μA/cm^2/mM, which was also an order of magnitude greater than the flat electrode. These results suggest that non-random nanotopography is a scalable and customizable engineering tool which can be integrated with Pt-BMGs to produce biocompatible biosensors with enhanced signal and sensitivity.

With the recent advancement of technologies to enable engineering of materials at the nanoscale and understanding cell-substrate interaction, the focus of biomaterials development is shifting from materials that are merely bioinert to engineering materials that are bioactive. Surface engineering enables the incorporation of additional functionality without compromising the bulk mechanical properties of a biomaterial [1]. By utilizing nanopatterning techniques, it is possible to engineer materials with novel surface properties to interact with and influence biological systems on the smallest relevant length scales – that of amino acids, proteins, and exosomes – in order to explore new frontiers in both the fields of materials and biology.

Bulk metallic glasses (BMGs) represent a novel class of materials that have significant potential for biomedical applications [2, 3]. Available in a range of compositions, bulk metallic glasses (BMGs) are amorphous metals, which are quenched rapidly to prevent crystallization. A quantitative measure of the glass forming ability of a metal is the critical cooling rate [4]. A sufficiently high critical cooling rate is required to bypass crystallization when cooling from a stable liquid phase in order to form a glass. Once in a glassy amorphous state, it is possible to form repeatable, complex, nanoscale structures using thermoplastic forming (TPF) by applying force once the temperature of the BMG alloy is elevated above the glass transition temperature, T_g [5-8]. Platinum-based metallic glass alloys (Pt-BMGs) are of particular interest because they

have been established to be biocompatible [3, 9], and platinum is also one of the target material used for biosensor electrodes [10]. By capitalizing on the TPF ability of Pt-BMGs, nanopatterned Pt-BMG substrates may be fabricated in air at comparably low processing temperatures less than 300°C [11].

Nanopatterned Pt-BMG substrates provide an ideal materials platform to engineer desired surface properties, such as enhanced surface area, without impacting the functionality of the bulk biomaterial. Previously, nanopatterned Pt-BMGs have been demonstrated for electrocatalysis applications, in which the BMG surface can be modified using both subtractive (dealloying) and additive (galvanic replacement) techniques [12, 13]. Such versatility positions nanopatterned Pt-BMGs for potential development as next generation biomaterials with both improved biocompatibility and device performance.

One challenge in the medical field impacting both individuals and healthcare systems is the metabolic disorder of diabetes. In 2014, 29.1 million American adults suffered from diabetes, which represents 9.3 percent of the population [14]. In patients with diabetes, blood glucose concentrations are often abnormally high, which may be caused by either increased insulin resistance or insulin deficiency. Blood glucose concentrations are ascertained by at-home testing using "test strip" electrochemical biosensors, which have known challenges with accuracy and repeatability [15 - 18]. The lack of reliable data on glucose levels complicates the patients' ability to respond, which leads to many patients living with inadequately controlled diabetes. Consequently, diabetes was the seventh leading cause of death in the United States in 2014 [19].

Glucose "test strip" biosensors, which are estimated to comprise approximately 85 percent of the entire biosensor market [10], produce an electrical current that is proportional to the amount of glucose in the blood. The electrical signal is generated via an electrochemical reaction that occurs when glucose in solution reacts with an enzyme, such as glucose oxidase, in the proximity of the electrode surface. In the case of glucose oxidase, the hydrogen peroxide byproduct is further reduced to generate a quantity of electrons proportional to the amount of glucose, as follows:

$$Glucose + O_2 \xrightarrow{Glucose\ Oxidase} Gluconic\ Acid + H_2O_2 \quad (1)$$

$$H_2O_2 \rightarrow H_2 + O_2 + 2e^- \quad (2)$$

Presence of nanotopography on a biosensor electrode can significantly increase effective sensing surface area with a given footprint. Increased effective surface area in turn enables greater amounts of enzyme to be attached directly to the electrode, which consequently may translate to increased sensitivity to changes in blood glucose levels. Heterogeneous surface area enhancements incorporated as additional elements to glucose biosensors have demonstrated the potential for improved biosensing [20 - 24], as has increased electrode surface roughness via texturing [25, 26]. However, integration of nanoscale structures also poses challenges, which may limit access to the additional surface area, such as stiction, clumping, and increased electrical interfacial resistance [27, 28]. The formation of nanotopography onto a planar electrode structure also results in a mechanical interface, which poses challenges related to the robustness of the interfacial adhesion strength and therefore causes device reliability concerns [21, 28, 29]. Reliability concerns are also a factor for nanotopography that is non-uniform and

highly variable; complex fabrication and testing processes requiring controlled environments also lead to issues [30]. Biocompatibility and safety of surface area-enhanced electrodes is also a critical consideration. Nanopatterned electrodes fabricated with hazardous substances such as arsenic are not viable, regardless of biosensing capability and potential manufacturability [29]. Transitioning to homogenous, high aspect ratio, nanoscale topography that is integrated into the base electrode without an interface between nanotopography may further enhance biosensor signal and sensitivity.

Taken together, the potential of Pt-BMGs as a biomaterial and novel processing ability presents an opportunity to apply the high surface area of nanopatterned bulk metallic glass substrates for biosensing applications. Work presented here utilizes nanopatterned Pt-BMG electrodes produced using TPF to explore the impact of ordered enhanced surface area on electrochemical biosensor performance for glucose detection.

METHODS:

Nanopatterned Pt-BMG Electrode Fabrication – Casting of the platinum-based $Pt_{57.5}Cu_{14.7}Ni_{5.3}P_{22.5}$ BMG alloy (Pt-BMG) from high-purity raw platinum, copper, nickel, and phosphorus was performed as described previously [4, 11]. The bulk Pt-BMG alloy was saw-diced into cylindrical samples approximately 2 mm in diameter and 3 mm in height; the samples were then cleaned ultrasonically in acetone followed by isopropanol. Thermoplastic forming (TPF) of the Pt-BMGs was carried out on a uniaxial compression load cell (Instron Model 5569) with a maximum applied force of 25 kN at 270ºC in air in order to produce the electrode surface nanotopography. Commercially available nanoporous alumina (Al_2O_3) membranes with a

nominal pore size of 200 nm (Whatman) were used as templates for the TPF process. After TPF, the Pt-BMG substrates were immersed in a solution of 30 percent KOH for 3 hours to dissolve the alumina molds. Following removal of the alumina templates, the nanopatterned Pt-BMG electrode structures were cleaned with acetone followed by isopropanol.

Structural Characterization – Prior to functionalization, the nanopatterned Pt-BMG electrodes were inspected and imaged using FIB-SEM as described previously [9]. Briefly, samples were cleaned with acetone followed by isopropanol and air-dried. Scanning electron microscope (SEM) images were obtained with the aid of a Hitachi SU-70 microscope. A subset of the samples used for SEM analysis was used to obtain focused ion beam (FIB) cross sections. A dual-beam FIB (FEI NanoLab 600 Dual Beam FIB) was used to mill cross sectional cuts into the Pt-BMGs in order to measure nanorod height.

Enzyme Functionalization Process – The nanopatterned Pt-BMG electrode substrates were functionalized with glucose oxidase enzyme [31]. Prior to functionalization, Pt-BMGs were washed with acetone and IPA for 5 minutes each, followed by two washes in phosphate buffered saline (PBS) for 5 minutes each. After washing, the Pt-BMG substrates were immersed in a solution of aminopropyltriethoxysilane (APTES) 10% (v/v) (Sigma Aldrich) in PBS for 10 minutes; the nanopatterned Pt-BMGs were then washed three times in PBS using a shaker table for agitation. Next, the Pt-BMG substrates were immersed in a 1% (v/v) glutaraldehyde solution (Sigma Aldrich) in PBS for 5 minutes, followed by three washes in PBS. Finally, the nanopatterned Pt-BMG electrodes were then placed in a 1 mg/ml glucose oxidase solution in 50 mM sodium acetate buffer (pH 4.0) (Sigma Aldrich) and allowed to dwell for 12 to 36 hours stored at 4°C.

Contact Angle Measurements – Prior to completing contact angle measurements, the Pt-BMG substrates were cleaned with acetone followed by isopropanol for 5 minutes each. The Pt-BMGs were then placed on the leveled stage of a custom-built contact angle measurement apparatus. A 5μL droplet of DI water was manually applied to the Pt-BMG substrate at the mid-radius locations using a micropipette. After 5 seconds, an image of the water droplet in profile on the Pt-BMG sample surface was captured. The contact angle was measured using Thorlabs uc480 Viewer application.

Electrical Property Characterization – Sheet resistance and electrical resistivity of the Pt-BMG alloy were obtained via 4-point probe measurements. For the electrical property measurements, Pt-BMG sheet samples were fabricated by TPF to produce samples approximately 100μm thick. The 4-point probe measurements were conducted using a Magne-Tron M-700 system at 1mV/100mA. Measurements were taken using both forward and reverse bias.

Electrochemical Characterization – Electrochemical performance of the Pt-BMG biosensor electrodes was characterized in three different test laboratories. For CV & AV testing in both labs, a three-electrode system was utilized, including a Pt-mesh counter electrode and an Ag/AgCl reference electrode. Testing was carried out using a BioLogic VMP3A potentiostat system and CHI model 840B & 1010A electrochemical analyzers. Prior to testing, PBS was exposed to a N_2 purge for 30 minutes. A magnetic stir bar was used at the bottom of the glass test vessel to maintain homogeneity. For the CV measurements, applied voltage was swept from 0V to 1V using both forward and reverse bias. For the AV measurements, 0.6V was applied, with a glucose concentration range of 2mM to 10mM.

RESULTS:

Bulk Metallic Glass & Surface Area Enhancement –

In this work, nanopatterned electrodes were fabricated in the form factor of nanorods with 200 nm nominal diameters on $Pt_{57.5}Cu_{14.7}Ni_{5.3}P_{22.5}$ Pt-BMG substrates utilizing TPF (Figure 1A). The nanorod arrays consisted of a roughly hexagonal symmetry with a spacing between nanorods of approximately 200 nm, referred to as a pitch ratio of 2:1; the exact form-factors were dictated by the patterns of the commercially available alumina templates. Extensive characterization of the nanopatterned substrates using SEM measurements determined the average nanorod diameter, *D*, was 247 nm, with a nanorod pitch of 440 nm. Average nanorod height of the Pt-BMG nanorods, *H*, was determined using FIB-SEM microscopy to be 3210 ± 109 nm for nanorods formed with an applied force of 25kN [9], resulting in an average nanorod aspect ratio of 13:1 (Figures 1B – 1D). Based off of these measurements, the surface area of a representative single nanorod is 2.538 um^2. Nanorods of such form factors in a hexagonal array result in an increase in effective surface area of 15.9X for a nanopattern unit cell vs. a flat equivalent electrode surface area, according to the following:

$$A_{Nanopattern\ Unit\ Cell} = \left[\frac{1}{2}(2D)(D\sqrt{3})\right] + \left[\frac{1}{2}\pi DH\right] \quad (3)$$

As a basis for comparison, nanopatterned Pt-BMGs were formed using a reduced applied force of 7kN during the TPF process. Using the same SEM measurement methods, the nanorods produced using reduced applied force demonstrated a decreased height, as anticipated. The average height was 1306 nm, with a measured surface area of 1.061 um^2 per nanorod.

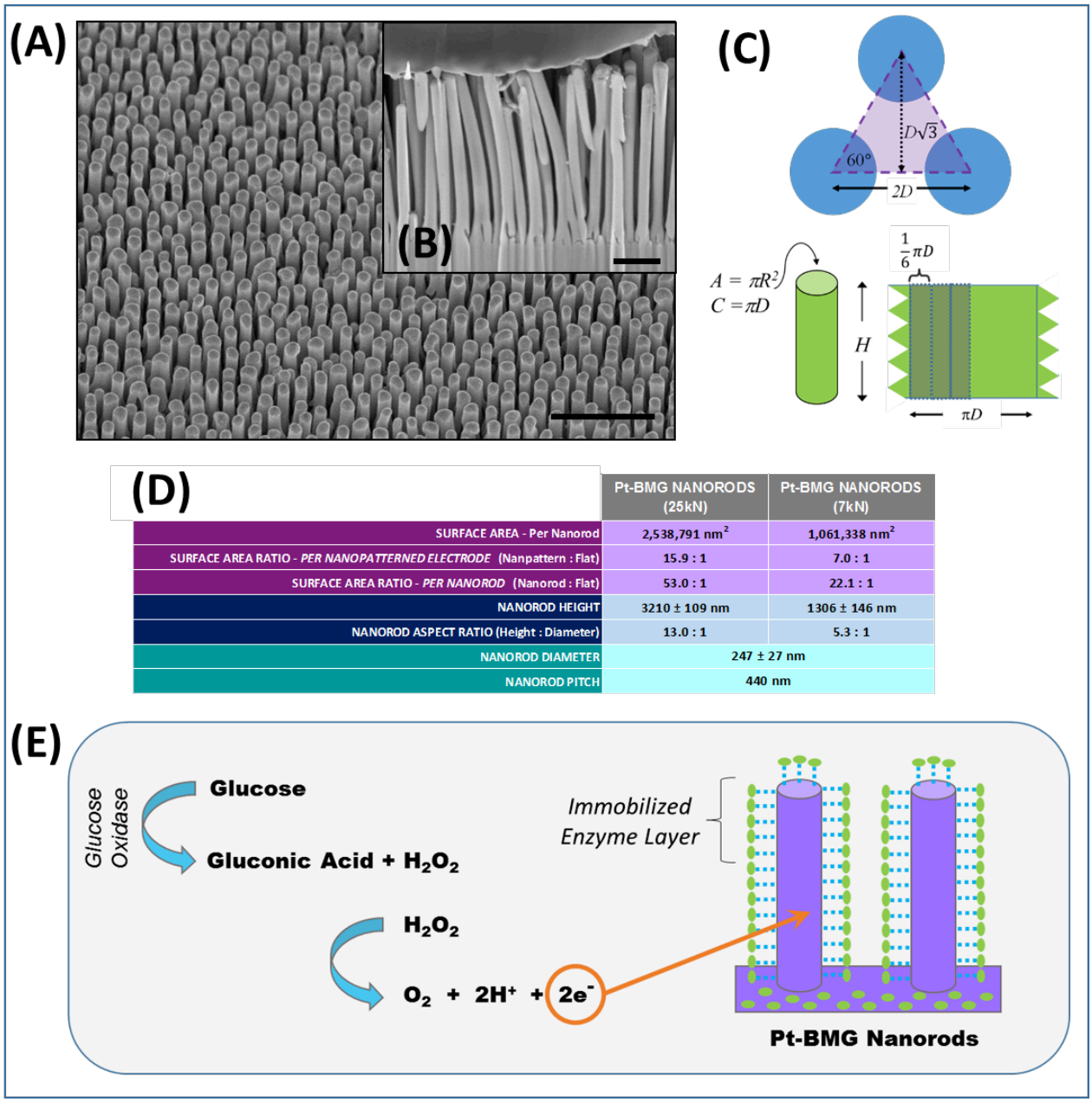

(D)

	Pt-BMG NANORODS (25kN)	Pt-BMG NANORODS (7kN)
SURFACE AREA - Per Nanorod	2,538,791 nm^2	1,061,338 nm^2
SURFACE AREA RATIO - *PER NANOPATTERNED ELECTRODE* (Nanpattern : Flat)	15.9 : 1	7.0 : 1
SURFACE AREA RATIO - *PER NANOROD* (Nanorod : Flat)	53.0 : 1	22.1 : 1
NANOROD HEIGHT	3210 ± 109 nm	1306 ± 146 nm
NANOROD ASPECT RATIO (Height : Diameter)	13.0 : 1	5.3 : 1
NANOROD DIAMETER	247 ± 27 nm	
NANOROD PITCH	440 nm	

Figure 1. Surface area impact on sensor sensitivity & signal for nanopatterned Pt-BMG biosensor electrodes. (A) Representative SEM image of a homogeneous nanorod array with a 200nm nominal nanorod diameter on a nanopatterned Pt-BMG biosensor electrode fabricated using thermoplastic forming. (B) Representative SEM image of post-FIB cross-sectional cut of a 200nm Pt-BMG substrate illustrating individual nanorod height. (C) Geometric representation of

nanorod surface area calculations. (D) Nanorod dimensions based on SEM & FIB analysis of Pt-BMG nanorods for radius, *R*, diameter, *D*, and height, *H,* were used to calculate nanorod aspect ratio and surface area theoretical estimates using measurement data, assuming hexagonal symmetry of the nanorod layout. (E) Graphical representation depicting a portion of each Pt-BMG nanorod functionalized with glucose oxidase enzyme and the resulting reduction-oxidation biosensing reaction when glucose is present. Scale bars, 2 μm (A); 1 μm (B).

The electrical properties of the Pt-BMG also provide a benefit for use as a biosensor electrode material. Electrical resistivity of bulk thermoplastically formed Pt-BMG was measured to be 202.8 μΩ-cm, with a sheet resistance of 0.0270 Ω/square, which is comparable to materials used in traditional semiconductor processing [32]. These values show that the Pt-BMG bulk material demonstrates sufficiently low resistivity for feasible use as a biosensor electrode material.

Pt-BMG nanorods therefore enhance the sensor performance in two ways: by providing additional surface area within a given base electrode footprint without a corresponding electrical or mechanical interface to produce greater electrical signal, as well as directly detecting the electrical signal in the immediate proximity where it is generated. Additionally, the TPF process produces electrode structures in which the material composition of the nanorods is consistent with that of the bulk electrode. The absence of an interface between the nanotopography and bulk electrode results in a lack of interfacial resistance, which may contribute to reduced latency of the biosensor signal, plus increased interfacial strength to improve device reliability.

Enzyme Functionalization & Validation –

To utilize the increased effective surface area for biosensing, the bulk electrode and exposed nanorod surfaces were functionalized with a bioactive enzyme [31]. In this case, glucose oxidase enzyme was selected to detect glucose since it is a widely-studied enzymatic reaction. In order to immobilize glucose oxidase on the BMG electrode surface (Figure 2A), a silanization procedure was performed to generate amine groups on the exposed nanopatterned electrode surfaces. Covalent coupling of glutaraldehyde to alkyl amine groups was then completed to create attachment sites for the glucose oxidase enzyme.

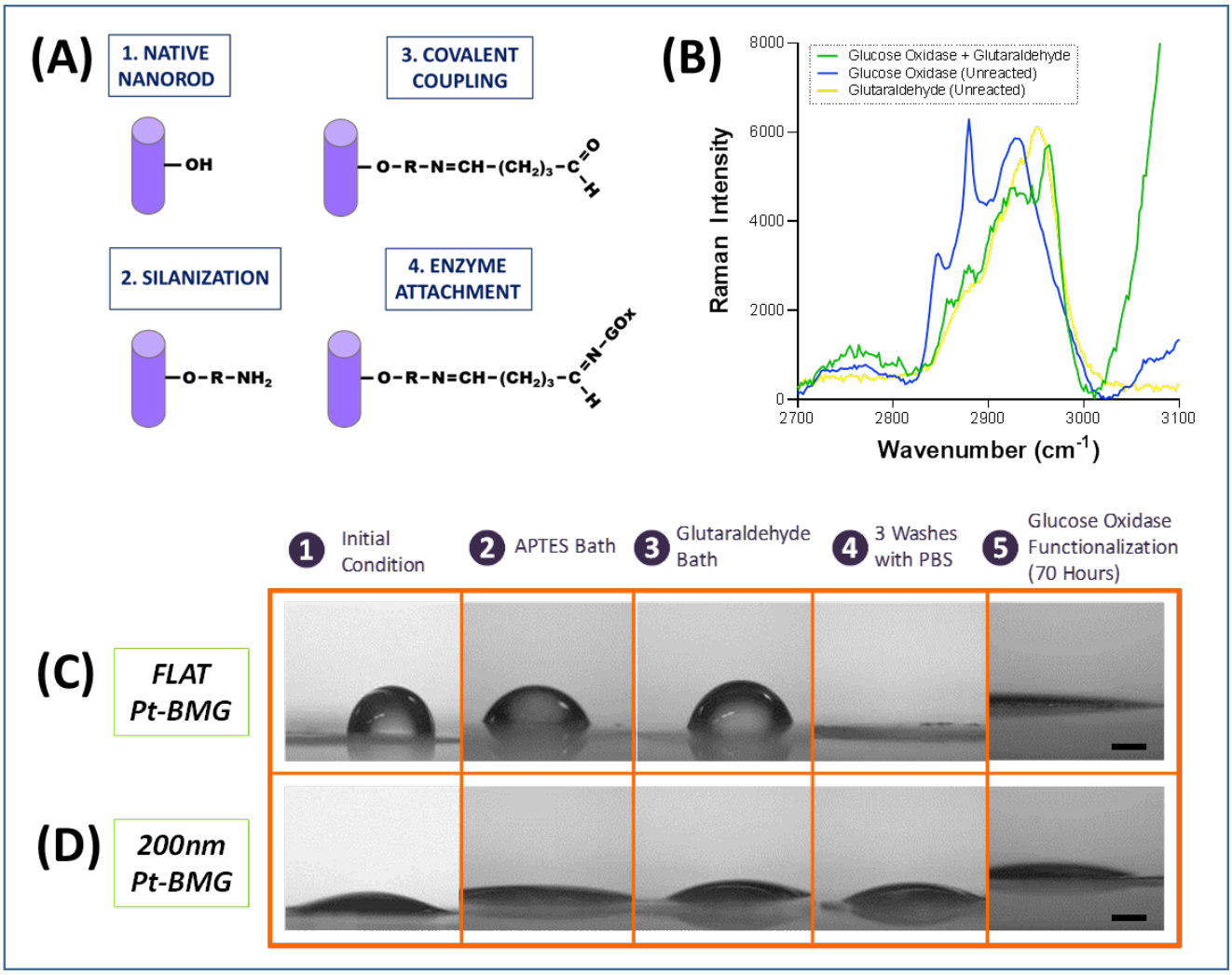

Figure 2. Glucose oxidase enzyme functionalization and process validation on Pt-BMG biosensor electrode surfaces. (A) Schematic illustrating the functionalization process for attaching glucose oxidase enzyme onto the Pt-BMG nanorod surface in which the following steps occur: 1. Beginning with Pt-BMG, a native hydroxide group is present on the exposed nanopatterned electrode surfaces; 2. After immersion in 10% aminopropyltriethoxysilane solution as part of the silanization process, amine groups are generated on the exposed electrode surfaces; 3. Covalent coupling of glutaraldehyde to alkyl amine groups occurs during a glutaraldehyde bath; 4. Glucose oxidase enzyme is attached to the Pt-BMG. The functionalization process was verified by using two analytical methods: Raman spectroscopy (B) and contact angle measurements (C & D). The evolution of the functionalization process was captured using Raman spectroscopy as glucose oxidase enzyme and glutaraldehyde reacted directly on the 200nm Pt-BMG nanopatterned substrate. Contact angle measurements using DI water droplets on both (C) Flat Pt-BMG and (D) 200nm Pt-BMG samples formed with 25kN of force throughout the various steps of the glucose oxidase enzyme functionalization process, which demonstrated hydrophilicity for both flat and nanopatterned Pt-BMGs. Scale bars, 1mm (C); 1mm (D).

Validation of the functionalization process was carried out via both Raman spectroscopy and contact angle wettability measurements to confirm that the solutions for the multiple steps of the glucose oxidase functionalization process reacted with the exposed electrode surface area. Raman spectroscopy, which is an ideal characterization method for optically opaque substrates, was used to observe the reaction of the compounds associated with the functionalization process *in situ* on the nanopatterned Pt-BMG electrodes (Figure 2B).

Contact angle measurements were also used to quantify the impact of functionalization process on the bulk Pt-BMG material properties. As depicted in Figures 2C & 2D, an initial hydrophilic state was observed for the Flat BMG control, with a superhydrophilic initial state seen for the nanopatterned Pt-BMG electrode substrates formed with the maximum applied force. Confirmation of superhydrophilic wetting behavior for the nanopatterned Pt-BMGs throughout the subsequent steps of the functionalization process suggest that the wet chemistries associated with the functionalization process successfully interacted with the additional nanorod sidewall surface area. Hydrophilic wetting behavior was observed throughout the entire functionalization process for the Flat BMG control as well. The increase in glucose oxidase enzyme loading on the nanopatterned electrodes was estimated to correlate with the 15.9X calculated increase in surface area.

Contact angle results observed here are consistent with the Wenzel criteria for wetting, which predicts that surface roughness as constituted by nanotopography will increase hydrophilicity on a surface that exhibits hydrophilic wetting in a non-rough state [33, 34]. Additionally, the contact angle measurements serve as a proxy to quantify the ability of the solutions for the functionalization process as well as the glucose-containing test solution to penetrate space between the nanorods to actively access the additional surface area [35]. An increase in electrode effective surface area is insufficient to improve signal and sensitivity if the required solutions to enable the electrochemical reaction are unable to access the additional surface area due to clumping or limited space between the individual nanorods.

Nanopatterned Pt-BMG Glucose Biosensor Electrical Performance –

The impact of the increase in effective surface area on nanopatterned Pt-BMG electrodes functionalized to detect glucose was quantified using cyclic voltammetry (CV) and amperometric voltammetry (AV). For both electrochemical tests, a three-electrode system was utilized, including a Pt-mesh counter electrode and an Ag/AgCl reference electrode, in addition to the nanopatterned Pt-BMG working electrode. To control the base surface area of the working electrode, a custom sample holder with a diameter of 1cm was fabricated using 3D printing to minimize sample-to-sample variation. An initial PBS solution was exposed to a nitrogen purge for 20 minutes prior to any electrical measurements. For the CV measurements, the applied voltage was swept from 0V to 1V a total of three times per measurement. In the case of the AV measurements, a constant voltage of 0.6V was applied to the working electrode. Concentrated glucose solutions were dosed in 2mM increments up to 10mM into the base PBS solution; this range of glucose concentrations was selected due to the scope of human blood glucose range.

Nanopatterned biosensors displayed an increase in the dynamic range of the current density for 200nm Pt-BMG vs. Flat BMG samples during the CV measurements. Since the current density values for the nanopatterned samples take into account only the cross sectional area of the base electrode rather than the additional surface area provided by the nanotopography, the resulting measurements are reported as effective current density. As shown in Figure 3, the effective current density for the 200nm Pt-BMG was 10-12X greater than that of the Flat BMG control, with the former exceeding current densities of 500 μA/cm^2. Repeatability and stability were demonstrated for both the nanopatterned BMG & Flat BMG samples at 0.6V, which was selected as the applied voltage for the subsequent AV measurements. Additionally,

the threshold voltage for switching between reduction and oxidation for both the Flat and 200nm Pt-BMG samples was determined to be approximately 0.1V.

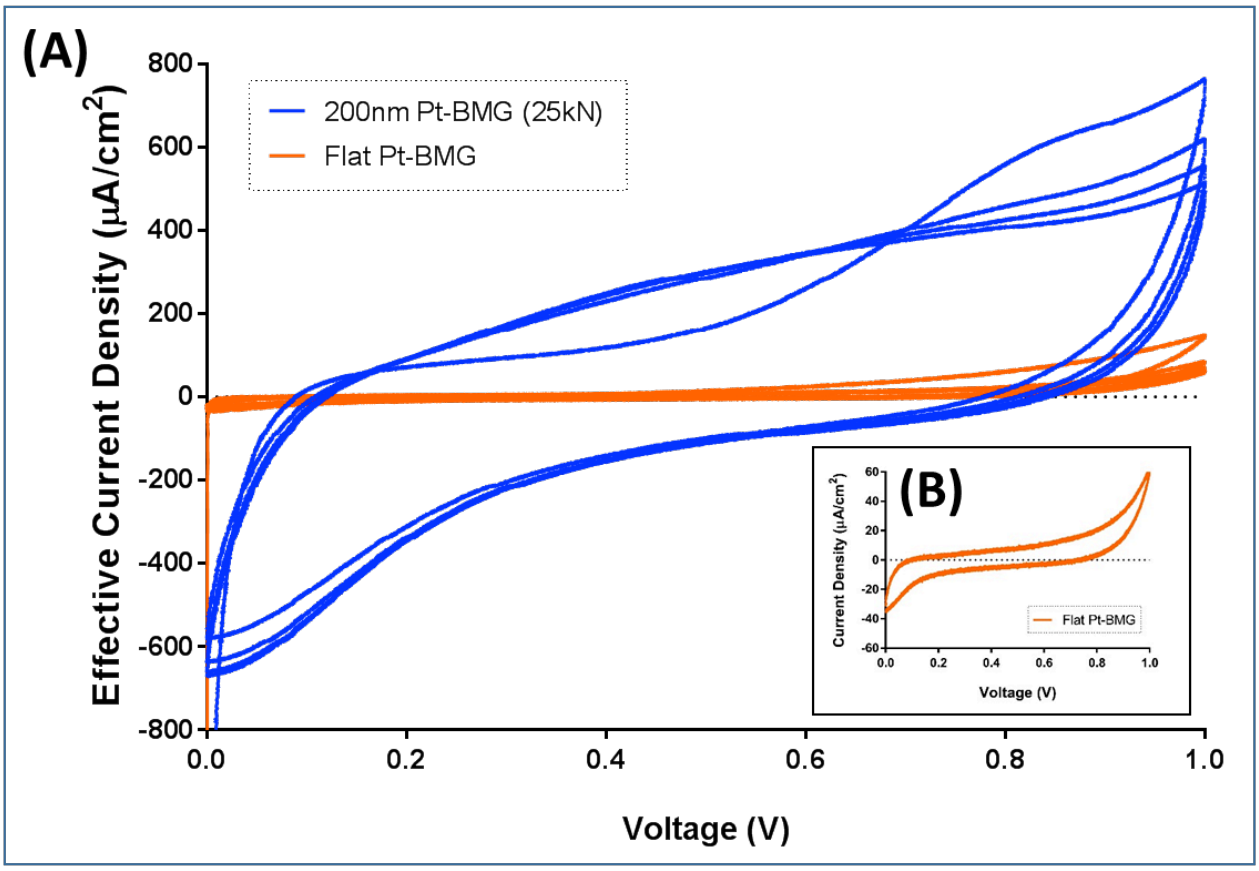

Figure 3. Impact of surface area enhancement on effective current density. (A) Comparison of the cyclic voltammetry (CV) curves for Flat Pt-BMG and 200nm Pt-BMG samples measured with an applied voltage ranging from 0V to 1V, with samples repeated in triplicate. The resulting effective current density was calculated based on a bulk electrode size of 1cm^2. (B) Magnified view of a representative Flat Pt-BMG electrode CV curve with current density presented on a reduced axis scale, illustrating steady-state performance at 0.6V and comparable current density to other planar flat electrodes reported in literature.

Benefits of the nanopatterned electrodes were also observed in the AV measurements, where the 200nm Pt-BMG samples formed with an applied force of 25kN demonstrated sensitivity to glucose approximately an order of magnitude greater compared to the Flat BMG controls (Figure 4). For measurements ranging from 0mM to 10mM glucose concentrations, the measured current density values ranged from 10 – 80 $\mu A/cm^2$ for 200nm Pt BMGs formed with 25kN, compared to <1 – 6 $\mu A/cm^2$ for the Flat BMG samples. As shown in Figure 4B, the nanopatterned BMG sensors exhibited a rapid response time. Dosing response was also highly linear; the linear correlation coefficients for all samples exceeded 0.988. Sensitivity values of 3.28$\mu A/cm^2$/mM and 0.348 $\mu A/cm^2$/mM were calculated for the 200nm Pt-BMG and Flat BMG electrodes, respectively.

The 200nm Pt BMG electrodes formed with a reduced applied force of 7 kN demonstrated glucose sensitivity of 1.17 $\mu A/cm^2$/mM, with current density values ranging from approximately 2 - 16 $\mu A/cm^2$. High linearity was also observed in the glucose dosing response for the 7 kN samples. Repeatability of AV measurements was also demonstrated across three different laboratory test platforms, as shown in Figures 4C – 4E, which illustrates stability of the Pt-BMG material and associated nanopatterning process.

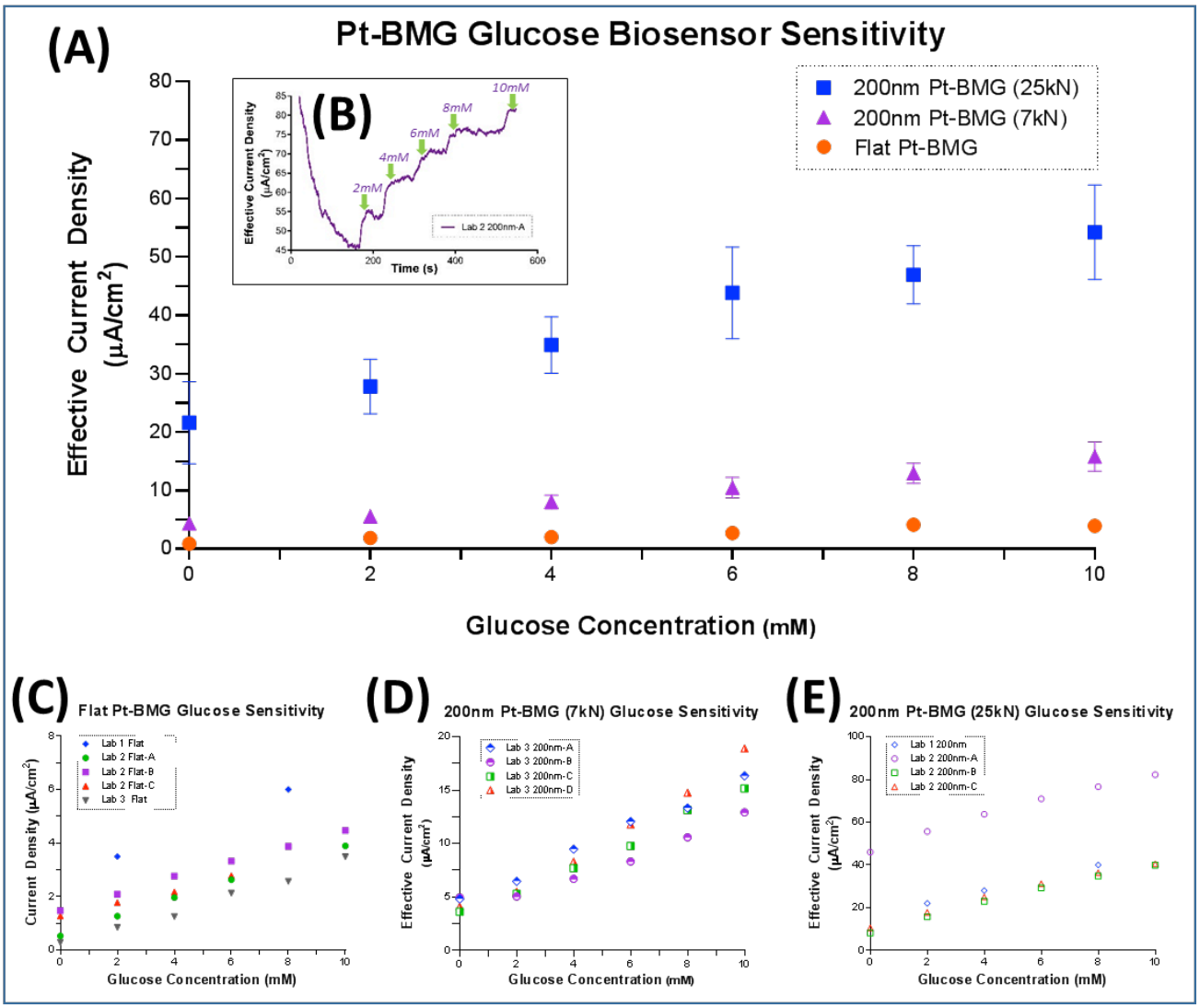

Figure 4. Enhanced signal and sensitivity induced by nanopatterned Pt-BMGs. (A) Quantification of the observed effective current density measurements for both nanopatterned and flat Pt-BMG electrode populations, in response to incremental glucose dosing experiments conducted across multiple test lab environments. (B) Real-time dose-response curve for a representative 200nm Pt-BMG biosensor electrode as the concentration of glucose in the solution was increased in 2mM increments. The response of individual samples demonstrated sufficient repeatability for both (C) Flat Pt-BMG electrodes, as well as 200nm Pt-

BMG electrodes thermoplastically formed at (D) 7kN and (E) 25kN of applied force to produce nanorods with an average height of 1306 nm and 3210 nm, respectively. All sample types were tested across multiple laboratory environments, denoted as Lab 1, Lab 2, and Lab 3, with individual samples of each type with multiple measurements denoted A, B, and C.

DISCUSSION:

The introduction of nanopatterning as a technique to enhance the available surface area for sensing on biosensor electrodes presents an opportunity to improve signal and sensitivity without negatively impacting the overall biosensor electrode size or increasing the complexity of the materials and interfaces in the biosensing system. Utilizing platinum-based bulk metallic glass as a platform for nanopatterned biosensor electrodes provides a material class with demonstrated biocompatibility and facile processing to produce repeatable nanopatterned electrodes for biosensing applications.

The order of magnitude increase in effective current density observed for the nanopatterned BMG electrodes evident from the CV results is consistent with the magnitude of the increase in effective electrode surface area reported herein. The effective current density dynamic range for the 200nm Pt-BMGs formed with 25 kN was 10 – 12X greater than that of the Flat BMG control. Compared with other published CV curves for planar glucose biosensors with similar applied voltages, the effective dynamic range of the 200nm Pt-BMG is also consistently an order of magnitude higher [36, 37]. A stable applied voltage range was observed from 0.3 to 0.7V for the nanopatterned Pt-BMG electrodes; such a broad stable voltage range is critical since the presence of high aspect ratio nanotopography has previously demonstrated

unreliable electrical results [28, 38]. While electrode material conductivity for the Pt-BMGs may also be a contributing factor, the significant dynamic range increase demonstrated by nanopatterned Pt-BMG CV measurements as compared to Flat BMG control signifies the potential for nanopatterning to improve biosensor performance.

The surface area increase for the nanopatterned Pt-BMGs was correlated with the observed order of magnitude increase in both signal and sensitivity corresponding to the AV measurements for the 200nm Pt-BMGs formed using both 25kN and 7kN applied force during the fabrication process as well. As anticipated, the 200nm Pt-BMGs formed with 7 kN of applied force which produced nanorods with reduced height – and therefore less surface area – yielded glucose sensing results with lower signal and sensitivity compared to the 200nm Pt-BMGs formed using the maximum applied force. Given the reduced bulk electrode diameter and increased center-to-edge variation in nanotopography height that are associated with reduced applied force during the TPF process, the observed results are sufficiently correlated with the reduction in nominal nanorod height.

With better manufacturing and process control techniques, the signal and sensitivity increase of 10 – 12X measured for the 200nm Pt-BMGs formed at 25kN would likely further approach the 15.9X surface area increase calculation. At present, the BMG nanopatterning accuracy is limited by the quality of the commercially available alumina molds; defects in the molds translate to nanorod geometry and spacing variability, which may result in nanorod clumping or inaccessible surface area for enzyme application or during glucose sensing. For both the Flat & 200nm Pt-BMG samples, AV measurements were completed on three different testing platforms. When sample-to-sample variation is also considered, the results from the multiple test facilities demonstrated acceptable repeatability and agreement.

In comparison to prior attempts to increase effective electrode surface area, the nanopatterned Pt-BMGs demonstrated comparable or greater increases in signal and sensitivity [21-25, 37-42]. Compared to commercially available glucose sensors, planar platinum electrodes, and comparable nanopatterned structures [21-23, 37-42], the nanopatterned Pt-BMGs exhibited signal and sensitivity that are also an order of magnitude higher. The lack of a physical or electrical interface between nanotopography and the base electrode in the case of the Pt-BMGs may be a contributing factor to the observed improvement. While one study utilizing extremely fine Pt-nanoparticles reported higher observed values for signal and sensitivity for glucose sensing [20], challenges may exist with repeatability and scalability of such nanoparticle structures. Similar challenges also exist for biosensors utilizing graphene-based nanoparticle coatings [24]. Embedding nanoparticles in a hydrogel or other matrix that is applied as a coating to a base electrode increases the sensor's structural complexity and introduces additional interfaces for the associated electrochemical signal to traverse prior to detection.

Non-enzymatic voltammetric and amperometric biosening methodologies for glucose detection involving nanotopography have garnered increased interest. While such methodologies may demonstrate potential increases in sensitivity, the ability to differentiate between variations in signals not produced by a specific biochemical reaction raises issues with scalability beyond a controlled laboratory setting [28, 29, 30]. Challenges with repeatability and required equipment sensitivity, which are not compatible with the constraints of real-world usage environments, may maintain the dependence on enzyme-specific biosensors.

Specifically for biosensors utilizing enzyme-based reactions, the surface area enhancement provided by nanopatterned Pt-BMG electrode surfaces offers an additional benefit of increased enzyme loading in immediate proximity to the biosensor electrode surface. When

the additional surface area of high aspect ratio nanorods is coated with active enzyme, the effect is an increase in the potential for a biochemical reaction to occur. In the case of glucose oxidase where hydrogen peroxide is produced, the increased surface area and associated presence of additional glucose oxidase creates increased opportunity for greater volumes of hydrogen peroxide to be produced and detected in the same close proximity to the biosensor electrode. Direct use of glucose is preferable to results obtained from dosing of H_2O_2 since a means of generating the correlating increased hydrogen peroxide volume may not exist directly on the sensor electrode.

In the case of nanopatterned Pt-BMGs, the low processing temperature for nanopattern fabrication and reduced precious metal content of the BMG alloys may facilitate ease of scalability. Potential benefits of such uniform, repeatable, nanopatterned surfaces may also motivate similar structures to be fabricated with existing industry-standardized semiconductor processing techniques. Additionally, many commercially available and experimental glucose sensors utilize benzoquinone (BQ) as an additive to amplify the electrochemical signal from glucose biosensors [21]; however, BQ is a toxic substance. Since the nanopatterned Pt-BMG results herein did not use any signal amplification method and Pt-BMG has been demonstrated to be a biocompatible material [3, 9], nanopatterned Pt-BMG biosensors may be conducive for additional work to explore use for *in vivo* biosensing applications.

CONCLUSION:

Enhanced surface area due to nanopatterning of Pt-BMGs leads to increased signal and sensitivity for biosensor electrodes compared to planar electrodes, with ten-fold increases achieved for both signal and sensitivity for glucose biosensing applications. The ability to

functionalize the Pt-BMG nanorods in conjunction with the bulk BMG substrate was demonstrated with glucose oxidase enzyme. The potential exists to functionalize the Pt-BMG nanorods with other enzymes, which creates opportunities for the broader application of nanopatterned Pt-BMGs as biosensors. Moreover, the electrical resistivity of Pt-BMG and increased surface area via nanopatterning demonstrate significant potential for increased signal and sensitivity for biosensing applications, and the lack of an interface between the nanotopography and base electrode structure improves nanopattern adhesion and durability.

AUTHOR INFORMATION

Corresponding Author

* Address correspondence to themis.kyriakides@yale.edu.

Author Contributions

The manuscript was written through contributions of all authors. All authors have given approval to the final version of the manuscript.

ACKNOWLEDGMENT:

Facilities used for this work were supported by Yale Institute for Nanoscience and Quantum Engineering and CRISP. The authors thank Ken Latzko and Peter Source of IBM Thomas J. Watson Research Center for tool access and support to complete four-point probe measurements. Additional thanks are offered to Mark Stalter and the IBM Semiconductor Research and Development Center in Fishkill, New York, for access to the FIB resource. The authors would

also like to thank Michael Kanik, Jittisa Ketkaew, and Tent Bordeenithikasem for contributions of time and effort related to the Pt-BMG alloy casting process. This work was primarily funded by CRISP (NSF MRSEC DMR 1119826) and National Institutes of Health Grant (GM-072194).

REFERENCES:

[1] Stevens, M. M.; George, J. H. "Exploring and Engineering the Cell Surface Interface." Science. 310 (2005), 1135–1138.

[2] Zberg, B.; Uggowitzer, P. J.; Loffler, J. F. MgZnCa Glasses without Clinically Observable Hydrogen Evolution for Biodegradable Implants." Nature Materials. 8 (2009), 887 – 891.

[3] Schroers, J.; Kumar, G.; Hodges, T.; Chan, S.; Kyriakides, T. "Bulk Metallic Glasses for Biomedical Applications." JOM. 61 (2009), 21–29.

[4] Schroers, J.; Johnson, W. L. "Ductile Bulk Metallic Glass." Physical Review Letters. 93 (2004), 255506, 1–4.

[5] Volkert, C. A.; Donohue, A.; Spaepen, F. "Effect of Sample Size on Deformation in Amorphous Metals." Journal of Applied Physics. 103 (2008), 083539, 1 – 6.

[6] Kumar, G.; Tang, H. X.; Schroers, J. "Nanomoulding with Amorphous Metals." Nature. 457 (2009), 868–872.

[7] Schroers, J. "On the Formability of Bulk Metallic Glass in Its Supercooled Liquid State." Acta Materialia. 56 (2008), 471–478.

[8] Jang, D. C.; Greer, J. R. "Transition from a Strong-Yet-Brittle to a Stronger-and-Ductile State by Size Reduction of Metallic Glasses." Nature Materials. 9 (2010), 215 – 219.

[9] Padmanabhan, J.; Kinser, E.; Stalter, M.; Duncan-Lewis, C.; Balestrini, J.; Sawyer, A.; Schroers, J.; Kyriakides, T. "Engineering Cellular Response Using Nanopatterned Bulk Metallic Glass." ACS Nano. 8 (2014), 4366–4375.

[10] Wang, Joesph. "Electrochemical Glucose Biosensors." Chemical Reviews. 108 (2008), 814 – 825.

[11] Pitt, E. B.; Kumar, G.; Schroers, J. "Temperature Dependence of the Thermoplastic Formability in Bulk Metallic Glasses." J. Appl. Phys. 2011, 110 (043518), 1–7.

[12] Doubek, G.; Sekol, R.; Li, J.; Ryu, W.H.; Gittleson, F.; Nejati, S.; Moy, E.; Reid, C.; Carmo, M.; Linardi, M.; Bordeenithikasem, P.; Kinser, E.; Liu, Y.; Tong, X.; Osuji, C.; Schroers, S.; Mukherjee, S.; Taylor, A. "Guided Evolution of Bulk Metallic Glass Nanostructures: A Platform for Designing 3D Electrocatalytic Surfaces." Advanced Materials. 2016, 28 (10), 1940 – 1949.

[13] Carmo, M.; Sekol, R.; Ding, S.; Kumar, G.; Schroers, J.; Taylor, A. "Bulk Metallic Glass Nanowire Architecture for Electrochemical Applications." ACS Nano. 4 (2011), 2979 – 2983.

[14] Centers for Disease Control and Prevention. "National Diabetes Statistics Report: Estimates of Diabetes and Its Burden in the United States, 2014." Atlanta, GA: US Department of Health and Human Services; 2014.

[15] Freckmann, G.; Baumstark, A.; Jendrike, N.; Zschornack, E.; Kocher, S.; Tshiananga, J.; Heister, F.; Haug, C. "System Accuracy Evaluation of 27 Blood Glucose Monitoring Systems According to DIN EN ISO 15197." Diabetes Technology & Therapeutics. 12 (2010), 221 – 231.

[16] Freckmann, G.; Schmid, C.; Baumstark, A.; Pleus, S.; Link, M.; Haug, C. "System Accuracy Evaluation of 43 Blood Glucose Monitoring Systems for Self-Monitoring of Blood Glucose according to DIN EN ISO 15197." Journal of Diabetes Science & Technology. 6 (2012), 1060 – 1075.

[17] Facchinetti, A. "Continuous Glucose Monitoring Sensors: Past, Present and Future Algorithmic Challenges." Sensors. 16 (2016), 2093.

[18] Obermaier, K.; Schmelzeisen-Redeker, G.; Schoemaker, M.; Klötzer, H.M.; Kirchsteiger, H.; Eikmeier, H.; del Re, L. "Performance Evaluations of Continuous Glucose Monitoring Systems: Precision Absolute Relative Deviation Is Part of the Assessment." Journal of Diabetes Science and Technology. 7 (2013), 824 – 832.

[19] Heron, M. "Deaths: Leading Causes for 2014." National Vital Statistics Reports. 65 (2016).

[20] Zhai, D.; Liu, B.; Shi, Y.; Pan, L.; Wang, Y.; Li, W.; Zhang, R.; Yu, G. "Highly Sensitive Glucose Sensor Based on Pt Nanoparticle/Polyaniline Hydrogel Heterostructures." ACS Nano. 7 (2013), 3540–3546.

[21] Deshpande, D.; Khaing, A.; Varadan, V. "Development of a nanoscale heterostructured glucose sensor using modified microfabrication processes." Journal of Micro/Nanolithography, MEMS, and MOEMS. 7 (2008). 023005.

[22] Gajdzik, J.; Lenz, J.; Natter, H.; Hempelmann, R.; Kohring, G.W.; Giffhorn, F.; Manolovac, M.; Kolbc, D. "Enzyme immobilisation on self-organised nanopatterned electrode surfaces." Physical Chemistry Chemical Physics. 12 (2010), 12604–12607.

[23] Rong, L-Q.; Yang, C.; Qian, Q-Y.; Xia, X.H. "Study of the nonenzymatic glucose sensor based on highly dispersed Pt nanoparticles supported on carbon nanotubes." Talanta. 72 (2007), 819–824.

[24] Zhang, W.; Li, X.; Zou, R.; Wu, H.; Shi, H.; Yu, S.; Liu, Y. "Multifunctional glucose biosensors from Fe3O4 nanoparticles modified chitosan/graphene nanocomposites." Scientific Reports. 5 (2016), 11129.

[25] Vaddiraju, S.; Legassey, A.; Qiang, L.; Wang, Y.; Burgess, D.; Papadimitrakopoulos, F. "Enhancing the Sensitivity of Needle-Implantable Electrochemical Glucose Sensors via Surface Rebuilding." Journal of Diabetes Science and Technology. 7 (2013), 441 - 451.

[26] Variola, F.; Brunski, J.; Orsini, G.; Tambasco de Oliveira, P.; Wazen, R.; Nanci, A. "Nanoscale surface modifications of medically relevant metals: State-of-the-art and perspectives." Nanoscale. 3 (2011), 335 – 353.

[27] Wang, S.; Liu, K.; Yao, X.; Jiang, L. "Bioinspired Surfaces with Superwettability: New Insight on Theory, Design, and Applications." Chemical Reviews. 115 (2015), 8230 – 8293.

[28] Cherevko, S.; Chung, C.H. "Gold nanowire array electrode for non-enzymatic voltammetric and amperometric glucose detection." Sensors and Actuators B. 142 (2009), 216 – 223.

[29] Lua, L.M.; Zhanga, L.; Qua, F.L.; Lua, H.X.; Zhanga, X.B.; Wua, Z.S.; Sh Huana, S.Y.; Wanga, Q.A.; Shena, G.L.; Yua, R.Q. "A nano-Ni based ultrasensitive nonenzymatic electrochemical sensor for glucose: Enhancing sensitivity through a nanowire array strategy." Biosensors and Bioelectronics. 25 (2009), 218–223.

[30] Chen, J.; Wang, K.; Hartman, L.; Zhou, W. "H2S Detection by Vertically Aligned CuO Nanowire Array Sensors." J. Phys. Chem. C. 112 (2008), 16017–16021.

[31] Subramanian, A.; Kennel, S.; Oden, P.; Jacobson, K.B.; Woodward, J.; Doktycz, M. "Comparison of techniques for enzyme immobilization on silicon supports." Enzyme and Microbial Technology. 24 (1999), 26 – 34.

[32] Shen, H. Ramanathan, R. "Fabrication of a low resistivity tantalum nitride thin film." Microelectronic Engineering. 83 (2006), 206 – 212.

[33] Wenzel, R.N. "Resistance of Solid Surfaces to Wetting by Water." Industrial and Engineering Chemistry. 28 (1936), 988 – 994.

[34] Quéré, D. "Wetting and Roughness." Annual Review of Materials Research. 38 (2008), 71 - 99.

[35] Kim, B.S.; Shin, S.; Shin, S.J.; Kim, K.M.; Cho, H.H. "Control of Superhydrophilicity/ Superhydrophobicity using Silicon Nanowires via Electroless Etching Method and Fluorine Carbon Coatings." Langmuir. 27 (2011), 10148 – 10156.

[36] Parng, S.H.; Yin, C.H.; Lee, K.F.; Chen, C.S.; Chou, T.C.; Lee, H.C.; Lin, Y.J. "Effect of temperature and glucose concentration on a glass-based sensor for long-term stability Investigation." Journal of Micro/Nanolithography, MEMS, and MOEMS. 10 (2011), 013003.

[37] Cardosi, M.; Zuifang Liu, Z. "Chapter 13: Amperometric Glucose Sensors for Whole Blood Measurement Based on Dehydrogenase Enzymes." Dehydrogenases. 2012, 336 – 343.

[38] Wang, J.; Myung, N.; Yun, M.; Monbouquette, H. "Glucose oxidase entrapped in polypyrrole on high-surface-area Pt electrodes: a model platform for sensitive electroenzymatic biosensors." Journal of Electroanalytical Chemistry 575 (2005), 139–146.

[39] Lin, Y.; Lu, F.; Tu, Y.; Ren, Z. "Glucose Biosensors Based on Carbon Nanotube Nanoelectrode Ensembles." ACS Nano Letters. 4 (2004), 191 - 195.

[40] Forzani, E.; Zhang, H.; Nagahara, L.; Amlani, I.; Tsui, R.; Tao, N. "A Conducting Polymer Nanojunction Sensor for Glucose Detection." Nano Letters. 4 (2004), 1785 – 1788.

[41] Radisica, A.; Morcos, B.M.; Op de Beecka, M.; O'Callaghan, J.M.; Van Hoof, C. "Electrochemical Deposition of Platinum Interconnects on Flexible Biocompatible Substrates." MRS Proceedings. 1626 (2014).

[42] Na Young Shim, N.; Bernards, D.; Macaya, D.; DeFranco, J.; Nikolou, M.; Owens, R.; G. Malliaras, G. "All-Plastic Electrochemical Transistor for Glucose Sensing Using a Ferrocene Mediator." Sensors. 9 (2009), 9896 – 9902.

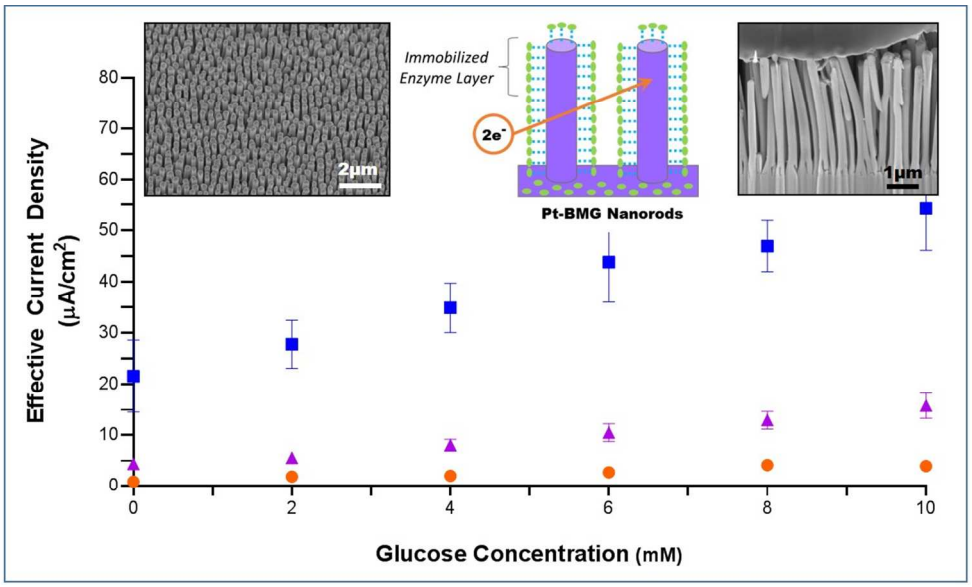

321x185mm (96 x 96 DPI)